COMPARISON OF CHIRP SCALING AND WAVENUMBER DOMAIN ALGORITHMS FOR AIRBORNE LOW FREQUENCY SAR DATA PROCESSING

A. Potsis[a], A. Reigber[b], E. Alivisatos[a], A. Moreira[c],and N. Uzunoglu[a]

[a] National Technical University Of Athens. Department Of Electrical And Computer Engineering
9, Iroon Polytexniou Str.GR -15780 Zografos, Athens, Greece, Tel/Fax (30)-10-7723694/7723557

[b] Technical University of Berlin, Photogrammetry & Cartography, Straße des 17. Juni 135, EB9
D-10623 Berlin, Germany, Tel.: ++49-30-314-23276, Fax.: ++49-30-314-21104

[c] German Aerospace Center (DLR) Institute for Radio Frequency Technology.
D-82230 Oberpfaffenhofen, Germany. Tel/Fax (49)8153-282367/281135

ABSTRACT

In recent years a new class of Synthetic Aperture Radar (SAR) systems, using low frequencies, have emerged. The combination of low frequencies with high bandwidths allows a variety of new applications. Several new fields arise in forestry, biomass estimation and in archaeological and geological exploration. The P-band SAR technology benefits from technological advances in antenna design, low noise amplifiers, band pass filters, digital receiver technology, as well as new processing algorithms [1], [2].

For all the new applications of an airborne P-band SAR system, the high-resolution imaging is an important parameter, but it cannot be easily achieved with conventional processing techniques. In this paper, the performance and limitations of the Extended Chirp Scaling (ECS) algorithm and wavenumber domain Omega-K processing algorithm are analysed and discussed. Additionally, modifications of both algorithms are proposed, which optimise the respective algorithm for processing low frequency, wide-beam and wide-band SAR data. Despite of the inherent limitations of the above mentioned processing algorithms, a deterministic phase error, called “digital phase error”, due to digital signal processing characteristics is formulated and its effect to the processed SAR data is analytically described. The analysis is carried out, using simulated low frequency airborne SAR data.

Keywords: Synthetic Aperture Radar -SAR, P-band SAR, Omega-K processor, Extended Chirp Scaling processing algorithm.

1. INTRODUCTION

An increasing amount of interest has evolved in VHF/UHF SAR applications. For most of the new applications high quality SAR data focussing is necessary. Although wavenumber domain processors are commonly used to process low frequency wide-beam and wide-band SAR data [1], they show certain limitations in performing a high-precision motion compensation of airborne SAR data. On the other hand, the Extended Chirp Scaling (ECS) algorithm [2] is proven to be very powerful in processing airborne data, but has limitations concerning long aperture synthesis and heavily squinted geometries. The limits of the along-track resolution of an airborne wide-band and wide-beam P-band SAR system are investigated in this first part of the paper, through the comparison of the performance of the ECS and Omega-K

* apotsis@esd.ece.ntua.gr, National Technical University Of Athens. Deprtment Of Electrical And Computer Engineering
9, Iroon Polytexniou Str.GR -15780 Zografos, Athens, Greece, Tel/Fax (30)-10-7723694/7723557

processing algorithms using simulated data. An efficient and robust correction algorithm, which compensates the errors introduced to the data due to ECS approximations, is addressed as well. A complete analysis of a deterministic phase error (digital phase error), introduced to SAR data processed by both algorithms, is illustrated at the end of the first part of the paper. The mathematical equation of the error is derived and several simulated results are presented as well. In addition, a detailed analysis of the motion compensation distortions related to the wide beam azimuth processing using both ECS and Omega-K algorithms is presented at the second part of this paper, using mainly simulated data sets in different motion errors scenarios.

2. ECS AND OMEGA-K ALONG TRACK RESOLUTION LIMITATIONS

The range resolution of a SAR system is determined mainly by the transmitted pulse duration and it can be easily adjusted. High along-track resolution in high frequency (more than 1 GHz) narrow-beam SAR systems is related mainly with the used processing algorithm. For wideband and wide azimuth beam SAR systems the along-track resolution is stretched to its fundamental limits.

According to [3] in the ideal data collection scenario, where no motion errors are introduced to the data, the Omega-K algorithm provides the exact solution in the focusing procedure, resulting in images with maximum possible along track resolution and minimum residual phase errors.

At lower center frequencies, where longer synthetic apertures and large integration angle are necessary to achieve high along track resolution, the ECS processing algorithm, due to approximations made in chirp scaling processing, does not provide the exact solution in the focusing procedure. As a result of this, the introduced phase errors are limiting the maximum achievable along track resolution.

According to [2], there are two approximations in chirp scaling processing. First, there is the Taylor approximation in wavenumber domain, which leads to SAR signal formulation in range-Doppler domain. This approximation is the basis for the chirp scaling processes. The second approximation is related with the lack of update of the "Secondary Range Compression" (SRC) with range during signal processing.

The phase error, arising from the first approximation, is mainly cubic with range frequency and causes an asymmetric range impulse response function and, as a result of this, an increase of the sidelobe level. In any case, the residual phase error, introduced to the peak position, is small compared to the corresponding phase error introduced by the second approximation.

Several methods for phase error compensation, caused by the approximations in the chirp scaling processing, can be found in the literature [4]. For the needs of our analysis, we apply an efficient and robust correction algorithms as analytically described in [5].

2.1 Simulated data analysis

A P-band raw data simulation has been performed to compare the performance of ECS and Omega-K algorithms in processing low frequency, high along-track resolution, wide-band and wide-beam SAR data. The main simulation parameters for both processing algorithms are listed in Table 1. As mentioned above, no motion errors have been introduced during raw data simulation. The simulated raw data set consists of three point targets, placed in near, middle, and far range (point targets 1, 2 and 3 respectively) of the processed scene.

The phase response of the three simulated targets in frequency domain is shown in Figure 1. No weighting function has been applied to the data (alpha=1.0). From this figure it becomes clear, that in the case where no motion errors are introduced to the data, the Omega-K algorithms results to ideal point target response where almost no residual phase errors are present (solid line plots). Nevertheless, the standard ECS processing algorithm, due to the above-mentioned approximations, introduces phase errors. From Figure 1 it can be concluded, that for 100Hz processed Doppler bandwidth (which corresponds to 1.0m azimuth resolution or alternatively $\pm 10^0$ processed squint angle), the maximum

residual phase error for far range point target is approximately 55^0 (doted line plots). The residual phase error is quadratic with range frequency, depends on the processed Doppler bandwidth and slant range.

According to [5], the error from the approximation $r_0 \approx r_{ref}$ (where r_{ref} is the chirp scaling reference range) after chirp scaling operation in wavenumber domain, can be expressed as:

$$E(f_a, f_r; r_0; r_{ref}) = \exp\left[j \frac{\pi \cdot f_r^{\,2}}{1 + a(f_a)} \cdot \frac{2 \cdot \lambda \cdot (\beta^2 - 1)}{c_0^2 \cdot \beta^3} \cdot (r_{ref} - r_0) \right] \tag{1}$$

Where $\beta(f_a) = \sqrt{1 - \left(\frac{f_a \lambda}{2v} \right)^2}$, $a(f_a) = \frac{1}{\beta(f_a)} - 1$, λ is the wavelength, f_a and f_r denote the azimuth and range frequencies, respectively, c_0 is the velocity of light, v is the mean velocity of the radar platform during data collection and r_0 is the distance to a point target at closest approach.

The error expressed by (1) can be corrected very efficiently by substituting the range frequency f_r by the maximum processed bandwidth MPB_r multiplied with a reduction factor F_r [5]. The reduction factor is dependent on the phase error at the end of the processed bandwidth and on the kind of weighting function [5]. The correction is only a function of azimuth frequency and slant range, and as a result of this it can be implemented in the azimuth compression stage of the chirp scaling processing without any additional computation effort. The correction can be expressed as [5]:

$$E_{corr}(f_a, r_0; r_{ref}; MPB_r) = \exp\left[j \frac{\pi \cdot MPB_r^{\,2} \cdot F_r}{1 + a(f_a)} \cdot \frac{2 \cdot \lambda \cdot (\beta^2 - 1)}{c_0^2 \cdot \beta^3} \cdot (r_{ref} - r_0) \right] \tag{2}$$

The simulated raw data set has been processed using the modified version of the ECS processor. The results are shown in Figure 1 (dash-dotted line). From this figure becomes evident that the modified version of ECS, which takes into account the approximations made in the chirp scaling processing, reduces the maximum residual phase errors for all simulated point targets to less than 10^0. Figure 2 depict the simulation results of point target 3 located in far range of the processed scene. The improvement achieved by the modified version of ECS is evident.

Parameter	Value
Wavelength	0.66601726 m
Range bandwidth	100, 50 and 25 MHz
Chirp duration	5 μs
Sampling frequency	100 MHz
PRF	500 Hz
Velocity	93.0827 m/s
Azimuth resolution	1m
Hamming weighting	a=1.0
Motion Errors	Not simulated

Table 1: Main parameters for P-band raw data simulator.

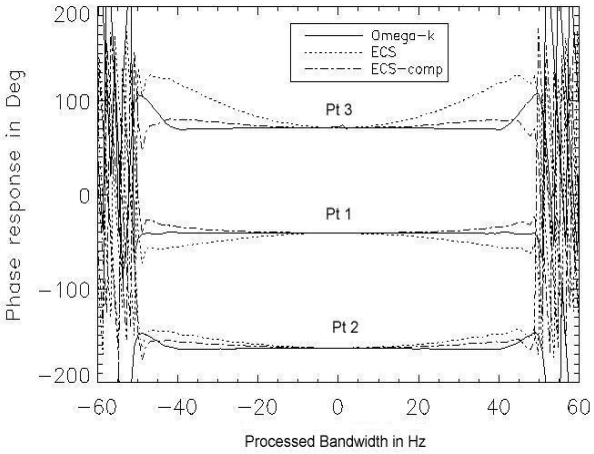

Figure 1: Phase response in frequency domain of three simulated point targets located in near (Pt1), middle (Pt2) and far range (Pt3) of the processed scene. After the correction applied in the standard ECS processing algorithm, the residual phase error reduce the minimum.

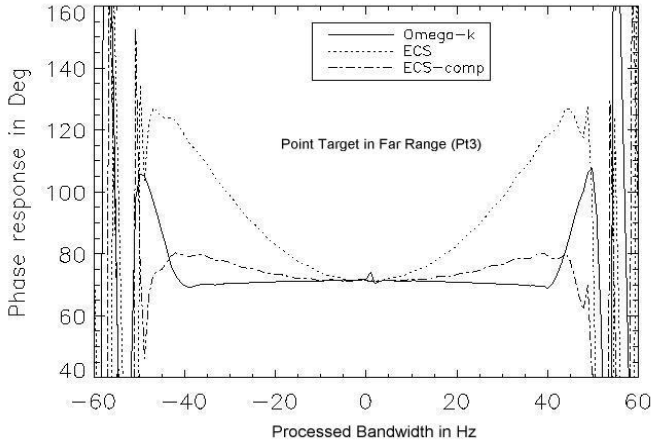

Figure 2: Phase response of simulated far range point target in frequency domain. The residual phase error reduces from 55^0 to less than 10^0 after the correction implemented at the standard ECS processing algorithm.

Recapitulating, when the standard ECS processor is used to process high-resolution low frequency SAR data, then the residual phase error, caused by approximations made in the chirp scaling processing, limits the maximum achievable along track resolution. In this case, a correction function, which compensates the error, is necessary. In the case where no motion errors are introduced to the data, the correction function significantly reduces the phase error, resulting in a response comparable to the ideal response of the Omega-K processing algorithm.

2.1.1 Digital mapping phase error

Despite the inherited phase errors of the two processing algorithms, as described above, the total residual phase error introduced to processed SAR data includes a deterministic digital mapping phase error. This digital phase error depends on the range distance between the target (position of the target's response maximum value, in a subpixel level) and the range distance where the digital mapping takes place as illustrated in Figure 4. As expected, a target that is positioned exactly in a range bin of the image has a zero digital mapping phase error. In the case where the target's range position differs from the image's range bins, which means that the target is located between two pixels in range, the digital phase error is non-zero and it is introduced to the analyzed data. In addition, the digital error grows, negatively or positively, as the subpixel shift of the target relative to the mapping range (range bin to be mapped) increase or decrease respectively. The effect of the digital phase error introduced to SAR data processed by both algorithms (Omega-K and ECS) is analyzed in the next paragraph, using simulated data.

- **Omega-K algorithm case**

In Figures 5 and 6 the digital mapping phase error of a point target response, which coincides with the residual phase error for the Omega-K processing algorithm, is presented for different positive or negative subpixel shifts of the maximum response of the simulated point targets respectively. A positive shift of a point target response corresponds to a backwards subpixel shift of the target response and a negative shift to a forward subpixel shift of the target, relative to the mapping range. The residual digital phase error, in the azimuth direction, of the Omega-K algorithm is given by the following equation [6]:

$$\phi_{\text{digital error}}(f_D) = -\frac{\lambda\pi}{2v^2}\cdot\Delta r\cdot f_D^{\,2} \tag{3}$$

where λ is the wavelength, v is the velocity of the sensor, $\Delta r = r_{map} - r_{target}$ (Figure 4) is the distance between the range of the target and the range bin being mapped and f_D is the doppler frequency. It must be noticed that the phase error has

a parabolic behavior. Actually this is an approximation of the phase error far from the bandwidth edges. There is a more exact expression at the bandwidth edges and equation 3 gets less capable to describe the phase error as the bandwidth processed in range increases.

Using equation 3, the digital phase error introduced to simulated low frequency SAR data processed by Omega-K algorithm for different subpixel shifts has been analyzed. A maximum phase error of 10 degrees, when no MoCo errors are introduced to the data (ideal case) has been measured.

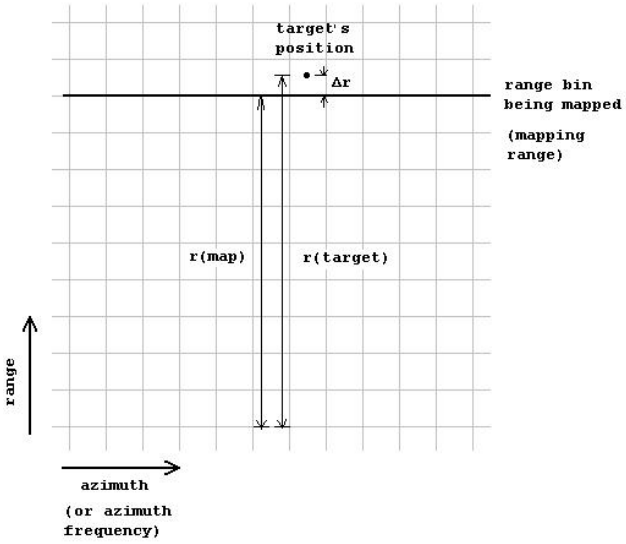

Figure 4: The processed grid of the data (cross sections of the horizontal with the vertical lines correspond to the pixels of the image). The range distance between the target (position of the target's response maximum value, in a subpixel level) and the range where the mapping takes place can be distinguished.

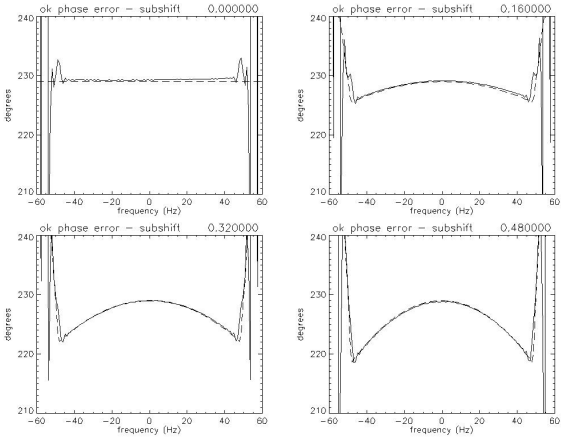

Figure 5: Phase response of a simulated point target in frequency domain using parameters of Table 1, with different subpixel shifts (16%, 32% and 48% of the range sampling interval) when the mapping range is greater than the real range of the target. The dashed line illustrates the theoretical phase error expressed by equation 3. From this figure becomes clear that the measured digital error coincides with the error calculated by equation 3.

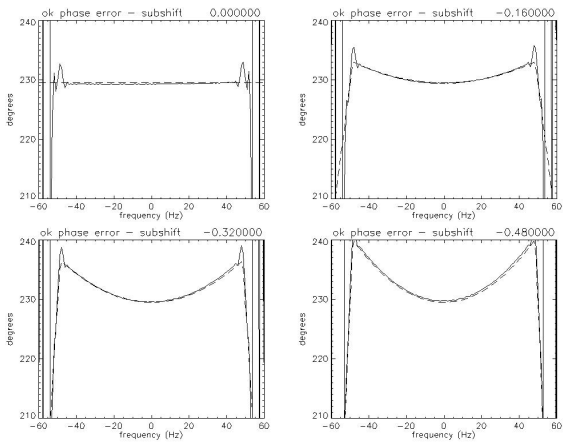

Figure 6: Phase response of a simulated point target in frequency domain using parameters of Table 1, with different subpixel shifts (16%, 32% and 48% of the range sampling interval) when the mapping range is smaller than the real range of the target. The dashed line illustrates the theoretical phase error expressed by equation 3. From this figure becomes clear that the measured digital error coincides with the error calculated by equation 3.

The digital mapping phase error is shown in Figure 5 (Figure 6) for positive (negative) subpixel shifts of 16%, 32% and 48% of the range sampling interval (the 0 subpixel shift corresponds to the case when the mapping range coincides with the target's range). Simulated data analysis proved that the measured digital phase error follows equation 3 with great accuracy and it gets negative when the mapping range is greater than the target's range and positive when the mapping range is smaller than the target's range. The digital error takes its maximum value when the subpixel shift approaches the 50% of the range sampling rate and as expected has the value of 10°.

- **ECS algorithm case**

The above-described digital mapping phase error appears, as expected, at SAR data processed by ECS algorithm, following equation 3. In this case it is caused by the difference of the azimuth focusing function at the target's range position with the actual mapping range. In the ECS processing case the digital phase error is introduced to processed data additionally to the inherent algorithm phase errors due to approximations in the chirp scaling algorithm, as described in the previous section of this paper.

Figure 7 illustrates the phase response of three simulated point targets in frequency domain located in near (7a), middle (7b) and far (7c) range respectively following the same analysis as for the Omega-K algorithm case of the previous paragraph. A positive subpixel shift of 16%, 32% and 48% of the range sampling interval has been performed and the introduced digital error has been calculated. The illustrated phase error consists of the ECS processing algorithm limitation error and the digital phase error. Finally, the digital mapping error that corresponds to current subpixel shift (Δr = k * (range sampling interval), where k = 0.16, 0.32, 0.48), as calculated using equation 3, is subtracted from the ECS residual phase error in the ideal case.

The inherent phase error of the ECS algorithm in the ideal case, after the subtraction of the digital mapping error is illustrated in Figure 7. It is obvious that the difference is constant and sufficient to characterize the extra phase error of the ECS against the Omega-K algorithm. With the dashed line, the ECS phase error subtracted by the digital mapping error is illustrated, at the specific subpixel shift. It can be observed that the difference between the two errors remains constant (50MHz processed bandwidth tin range). (a) Pt1, (b) Pt2, (c) Pt3. Additionally, the phase error of the targets located in the middle and the far range (Pt2 and Pt3 respectively) reduces as the shift increases. The reason for this effect is that for positive shifts the digital mapping phase error is negative (see Figure 5).

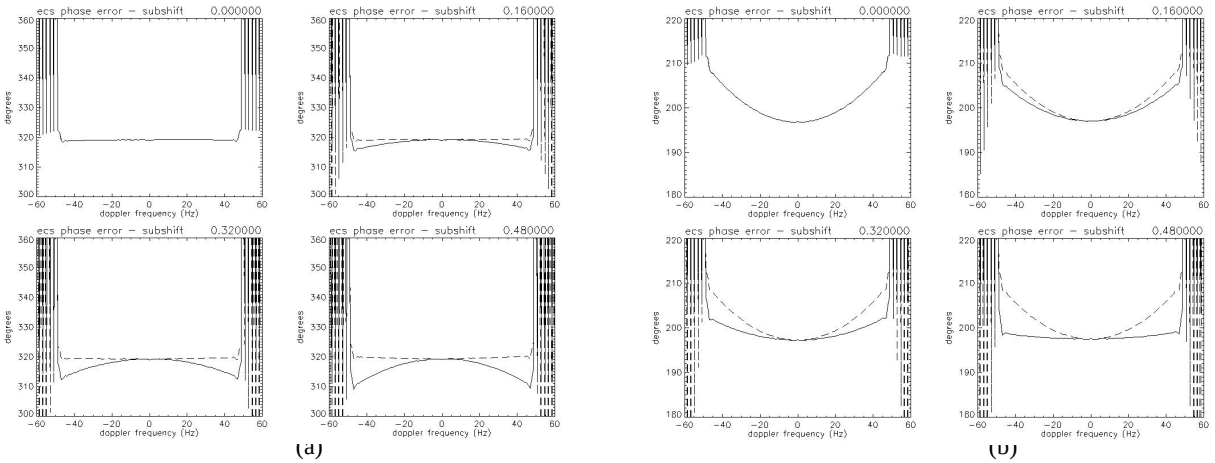

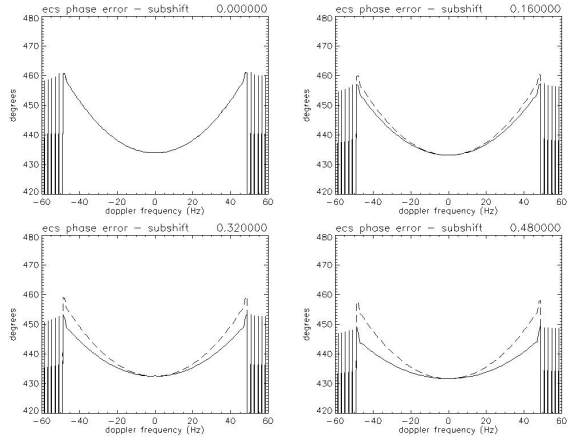

(c)

Figure 7: Phase response in the doppler frequency domain of the ECS algorithm for different distances (different subpixel shifts), between the range of the target (maximum of the target's response) and the mapping range. With the dashed line, the ECS phase error, subtracted by the digital mapping error at the specific subpixel shift, is illustrated. It can be observed that the difference between the two errors remains constant (50MHz processed bandwidth tin range). (a) Pt1, (b) Pt2, (c) Pt3. From this figure it can be concluded that the digital phase error effects negatively or positively the residual phase error introduced to SAR data due to ECS algorithm limitations and it must be always taken into account when analyzing SAR data processed by the standard ECS processor.

3. MOTION ERROR EFFECTS IN ECS AND OMEGA-K PROCESSORS

A crucial problem in most airborne SAR sensors is the compensation of motion errors, induced by atmospheric turbulence (i.e. the compensation of changes of the plat-form forward velocity vector in orientation and/or in mag-nitude). Airborne sensors, in contrary to spaceborne sensors, always show deviations from the ideal flight track. SAR imaging from such unstable platforms requires an accurate measurement of the antenna position during the flight and a modified processing scheme, which takes into account the non-linear movement of the sensor [2].

The Chirp Scaling (CS) algorithm [7] was developed mainly to avoid interpolations, which were necessary when we had to deal with strong range-cell migration data (i.e. when wide azimuth beam data have to be processed). A improved version of the CS was the ECS algorithm, which was developed originally for processing airborne data with strong motion errors (like the E-SAR Do-228 platform [8]) and variable Doppler centroid in range or/and in azimuth direction. According to [2], the ECS processing algorithm performs motion compensation in two steps. The first order motion compensation is defined as being the phase error correction for a reference range, and it is carried out directly with uncompressed raw data. After the range compression of the data has been performed, the motion compensation phase function is updated with range. This called second order motion compensation and it is performed right before the azimuth compression.

It has been demonstrated that motion errors up to some tens of meters can be compensated, in the case of the E-SAR system, using the ECS processor. Additionally, the implementation of a sub-aperture algorithm in the ECS algorithm, when it is used to process low frequency wide beamwidth SAR data, as described in [9], suppresses the residual motion compensation error to minimum possible extend. The combination of the ECS correction function, as described in the first part of this paper, with the sub-aperture correction, results to maximum possible along track resolution with a residual phase error comparable to the error illustrated in the ideal processing case of Fig. 1 and 2. In most of the operational examples, the remaining errors are strongly related with the accuracy of the navigation units (DGPS/INS/IMU) and not with the improved ECS motion compensation correction algorithm itself.

On the other hand, due to processing architecture of the Omega-K algorithm, a high precision motion correction cannot be applied in it. Compared with the ECS two-step motion compensation, in Omega-K only the first order motion error

correction can be applied [3]. The first-order MoCo is the range-independent part of the real MoCo, and is applied directly after range compression. The range-dependent part can only be applied after correction of the RCM, which is not possible in Omega-K.

The P-band raw data simulator has been used to compare the performance of ECS and Omega-K algorithms in processing low frequency, high along-track resolution and airborne SAR data with motion errors. The same simulation parameters of Table 1 have been used again, now adding one quarter of typical motion errors typically occurring in case of the E-SAR. The phase response of one simulated point target in frequency domain located in the center of the processed scene is shown in Figure 8. From this figure it becomes clear that, even in the case of small motion errors, the Omega-K algorithm fails to remove completely the introduced phase errors. The residual phase error is in the order of 45^0. On the other hand the modified ECS processor compensates most of the motion errors accurately, resulting in maximum possible along track resolution. It has to be noted that the first order MoCo correction of Omega-K has been optimized for the range distance of the target; in the general case even worse results can be expected.

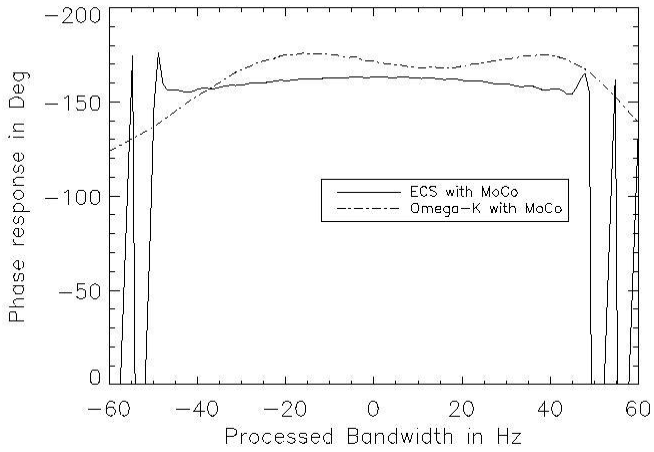

Figure 8: Phase response of one simulated point target located in the center of the processed scene, with motion errors in frequency domain. The Omega-K algorithm fails to compensate even small motion errors resulting to a maximum residual phase error of 45^0.

4. CONCLUSIONS AND FUTURE WORK

The limits of the along track resolution of an airborne wide-band and wide-beam P-band SAR system have been analyzed in this paper through the comparison of the performance of the ECS and Omega-K processing algorithms. Simulated data analysis proves that a correction function can be introduced to the ECS, which results in a focusing accuracy comparable with the ideal response of the Omega-K processing algorithm. Furthermore, the digital mapping phase error should be taken into consideration when an accurate estimation of the algorithm's residual phase error is desired. This deterministic phase error has been formulated and calculated using simulated low frequency SAR data in different processing scenarios, resulting in a maximum phase error of 10^0 for 1m azimuth resolution and 50MHz processed bandwidth in range.

In the case where strong motion errors are introduced to the data, the modified ECS processor compensates successfully most of the errors, even in the case of low frequency wide-band and -beam SAR data processing, resulting in maximum possible along-track resolution with minimum residual phase error. On the other hand, the Omega-K processor fails to compensate even small phase errors introduced by motion of the radar platform during data acquisition.

A modified version of the Omega-K processor, which combines its ideal point target response accuracy with the ECS motion compensation correction performance, is under development with quite promising results.

REFERENCES

1. L.M.H. Ulander, H Hellsten and G. Stenström: 'Synthetic-Aperture Radar Processing using Fast Backprojection', EUSAR'2000 3rd European conference on Synthetic Aperture Radar, Munich, Germany, pp. 753-756, 2000.

2. A. Moreira, J. Mittermayer and R. Scheiber: 'Extended Chirp Scaling Algorithm for Air- and Spaceborne SAR Data Processing in Stripmap and ScanSAR Imaging Modes' IEEE Transactions on Geoscience and Remote Sensing Vol. 34, No. 5, Sept 1996.

3. C. Cafforio, C. Prati and F. Rocca: "Full resolution focusing of SAESAT SAR images in the frequency wave number domain" International Journal of Remote Sensing, Vol. 12, No. 3, pp. 491-510, 1991.

4. G. W. Davidson, I. G. Gumming, and M. R. Ito: 'A Chirp Scaling Approach for Processing Squint Mode SAR Data'. IEEE Transactions on Aerospace and Electronic Systems, Vol. 32, No.1, pp. 121-133, January 1996.

5. J. Mittermayer, A. Moreira and R. Scheiber: 'Reduction of Phase Errors Arising from the Approximations in the Chirp Scaling Algorithm', Proceedings of IGARSS'98, Seattle USA, pp. 1015-1019, 1998.

6. E. Alivisatos, 'SAR digital signal processing', diploma thesis, June 2002, NTUA internal publications, Department Of Electrical And Computer Engineering, in press.

7. R. K. Raney, H. Runge, R. Bamler, I. Cumming, and F. Wong: "Precision SAR processing without interpolation for range cell migration correction" IEEE Transactions on Geoscience and Remote Sensing, Vol. 13, No. 5, pp. 991-998, 1992.

8. R. Horn: "The DLR Airborne SAR Project E-SAR." Proceedings of IGARSS'96, Lincoln, Nebraska USA. pp. 1624-1626, 1996.

9. A. Potsis, A. Reigber, J. Mittermayer, A. Moreira and N. Uzunoglou: 'Sub-aperture algorithm for motion compensation improvement in wide-beam SAR data processing'. Electronic Letters, Vol. 37, No.23, pp. 1405-1407, November 2001.